Adaptive Distance Learning Scheme for Diffusion Tensor Imaging using Kernel Target Alignment

P.R. Rodrigues[1], A. Vilanova[1], T.Twellmann[2], and B.M. ter Haar Romeny[1]

[1] Department of Biomedical Engineering, Eindhoven University of Technology, WH 2.103, 5600 MB Eindhoven, The Netherlands
P.R.Rodrigues@tue.nl
[2] MeVis Medical Solutions AG, Universitätsallee 29, 28359 Bremen, Germany

Abstract. In segmentation techniques for Diffusion Tensor Imaging (DTI) data, the similarity of diffusion tensors must be assessed for partitioning data into regions which are homogeneous in terms of tensor characteristics. Various distance measures have been proposed in literature for analysing the similarity of diffusion tensors (DTs), but selecting a measure suitable for the task at hand is difficult and often done by *trial-and-error*.
We propose a novel approach to semiautomatically define the similarity measure or combination of measures that better suit the data. We use a linear combination of known distance measures, jointly capturing multiple aspects of tensor characteristics, for comparing DTs with the purpose of image segmentation. The parameters of our adaptive distance measure are tuned for each individual segmentation task on the basis of user-selected ROIs using the concept of Kernel Target Alignment. Experimental results support the validity of the proposed method.

1 Introduction

Diffusion Weighted MRI [1] constitutes a valuable tool that allows a non-invasive look at fibrous structures. Among the most important applications of Diffusion Tensor Imaging (DTI) is the study of brain connectivity or of the fibrous structure of muscle tissue such as the heart [2,3]. DTI has also been used to identify subtle abnormalities in several diseases such as stroke schizophrenia and multiple sclerosis [4].

In DTI more than six gradient directions are scanned, enough to compute the *diffusion tensor* (DT) per voxel, representing the local pattern of directional tissue diffusivity. The diffusion tensor is represented by a 3×3 positive definite symmetric matrix $\mathbf{D}$. The diffusion coefficients in each direction $\boldsymbol{r}$ are given by $\boldsymbol{r}^T\mathbf{D}\boldsymbol{r}$.

A common way to visualise the tensor data (Vilanova et al. [2]) is by fiber tracking. Given the DT field, fiber tracking techniques try to reconstruct the fibrous structures (i.e., fiber tracts).

In several applications, such as comparison between subjects, it is interesting to segment structures at a higher semantic level, e.g. coherent white matter bundles such as the *corpus callosum*, [5–7]. It is also necessary to derive statistical properties of diffusion tensors (DTs) to identify differences in tissue morphology, e.g., between healthy and pathological areas [4]. For these reasons, clustering techniques have been used to group individual fiber tracts into coherent structures [8]. However these methods deal with derived structures from the tensor field (i.e., do not use directly the original full tensor information). Therefore they are very sensitive to the used fiber tracking method and the parameter setting of those. An alternative to clustering fibers is the direct segmentation of the tensor field in volumetric regions. These methods assume that tensors will belong to the same bundle if they are similar to each other. Several segmentation techniques have been presented in the last years [5–7, 9–11]. These techniques require the notion of (dis)similarity of two DTs, i.e., a measure which indicates when a tensor is considered to be similar enough to belong to the same region. Clearly, the segmentation results are highly dependent on the choice of measure. So here again the problem of how to define distance (or other dissimilarity measures) in the DTI codomain imposes itself. Different similarity measures for DTs have been introduced in the past. Alexander et al. [12] and Peeters and Rodrigues et al [13] extensively analysed the different (dis)similarity measures, which are of different nature and sometimes lack physiological significance. Therefore, it is difficult to predict which measure will give better, or similar results. The choice of measure depends on the application at hand. Usually an ad-hoc definition of parameter values and choice of similarity measures is used.

The contribution presented in this paper lies in the assessment of tensor field homogeneity characteristics by automatically determining a suitable parameterised similarity measure simultaneously capturing multiple aspects of tensor characteristics. The results of the presented method can then be used in any segmentation algorithm as, for example, region growing.

This problem of *metric learning* and parameter estimation has been addressed before in the machine learning and pattern recognition literature [14,15]. We extended these methods for the particular problem of diffusion tensor segmentation. With the proposed pre-processing distance learning algorithm, the parameters for a segmentation algorithm, Region Growing, are inferred from the data. A seeding region is selected (by the user) and the algorithm will segment the spatially connected 3D section with the diffusion tensors that are similar to the initial chosen region and dissimilar to the rest. The initially flexible learning scheme adapts itself to the task at hand. This technique can be used for different segmentation algorithms and for illustration we present the results using region growing.

2 Methods

The main goal of this work is to assess what distance or combination of distances better express the homogeneity characteristics of a structure defined in a tensor

field, e.g., the brain. The results of the distance/parameter learning are then used to drive a Region Growing segmentation algorithm (see Figure 1). The distance learning algorithm infers the distance(s) that best discriminates a selected Region of Interest (ROI) from the entire image volume represented by a random sample of DTs. The optimal combination of distances will then be used in the segmentation algorithm and a spatially connected volume of tensors is obtained. Then the user will be able to further improve the process by adding additional negative ROIs, i.e., examples of tensors that are different from the target region and provide complementary information.

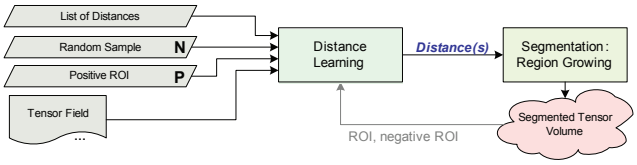

Fig. 1. Global gist of the distance/parameter learning and segmentation

Figure 2 shows the details of the distance learning algorithm. From the tensor field volume data we define a labeled set $\mathbf{S} = (\mathbf{D_i}, l_i)$ of n DTs $\mathbf{D}$ with a label l. The set S is defined as the union of two subsets of DTs: $\mathbf{P}$, a set of representative DTs from a user defined ROI (positive ROI), where $l = +1$; and $\mathbf{N}$, a set of representative DTs for the whole volume (negative ROI), where $l = -1$.

Distance matrices are constructed by calculating the distance between all pairs of tensors in the set $\mathbf{S}$. Each row is considered as a feature vector with the distance from a tensor to all others in the training set. From these feature vectors, symmetric matrices, referred to as kernel matrices (i.e., Gram Matrices), are calculated by computing all possible inner products between each vector. For a uniform behavior of the algorithm, without minding the scale, a normalisation of the individual kernel matrices is performed. Then, with a linear combination of the different kernel matrices, one per considered distance, we define a new kernel matrix $\mathbf{K}$ with a set of unknown parameters (the weights).

Using a grid search based method, the weights are estimated in order to maximize the Kernel Target Alignment measure described in Section 2.3. This maximum gives the best alignment between the kernel matrix $\mathbf{K}$ and an equally sized label matrix, i.e., which combination of distances provides the best discrimination for the considered data.

In the following, we describe the optimization of the kernel target alignment for the distance learning. In Section 2 several elements of the algorithm are introduced and in Section 3 experiments of the distance learning algorithm are presented.

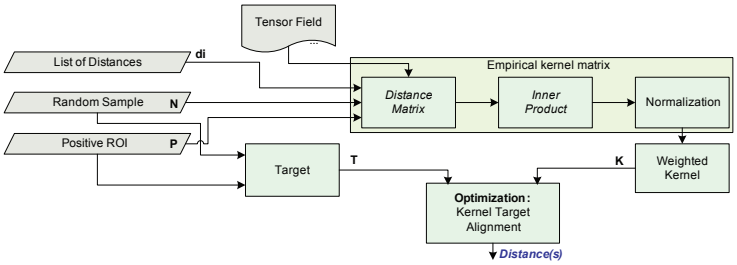

Fig. 2. Detailed scheme of the distance learning algorithm

2.1 Distances

A distance measure d has to be such that $d(\mathbf{A}, \mathbf{B})$ is small if tensors $\mathbf{A}$ and $\mathbf{B}$ are similar [13]. The distance learning algorithm does not require the distance to be a metric, the triangle inequality is not a requisite.

Distance measures convey different aspects of a diffusion tensor. While some capture changes in individual degrees of freedom (e.g., difference in anisotropy), others use the full tensor information. Thus their use is sometimes redundant, i.e., different measures describe common tensor attributes. There are measures that use the full tensor, like *Riemannian* based measures, that have a mathematical nature which does not have a direct intuition of the physiological meaning. Thus, the results are not that predictable. Other measures like the ones presented by Kindlmann et al [10] decompose tensor variations into changes in shape and orientation, covered by three invariant gradients and three rotation tangents. In this work, a tunable difference measure between two DTs is introduced. This measure uses a weighted sum of the individual measures. However, the definition of the weights depends on the task. Furthermore, this is only good for very small differences, since the invariant gradient and rotation tangent coordinate frame is not accurately defined for a large difference between tensors. Therefore, we do not use these measures.

In order to show the flexibility of our framework, we evaluate the following set of different distances [13]: difference of FA (ds_{FA}), difference of MD ds_{MD}, angular difference d_{ang1}, Frobenius distance d_{L2}, geometric distance d_g, Log-Euclidean distance d_{LE} and the symmetrized Kullback-Leibler d_{KL}. These measures are chosen because they are distances, $d(\mathbf{D_1}, \mathbf{D_1}) = 0$, symmetric and positive. Other similarity measures could be used, however they must be converted into a distance measure, see Haasdonk et al [16].

2.2 Empirical Kernel Matrices

The main idea of kernel methods is to map the input data (i.e. here distance between tensors) to a feature space provided with a dot product. The mapped data is then dichotomized. A kernel matrix for a measure m, can be regarded as

a pairwise similarity (i.e., an element is similar to itself, $m(A, A) = 1$) between all elements of a set, represented in a feature space.

A kernel matrix $\mathbf{K}$ for a set of L feature vectors can be regarded as a matrix of pairwise similarity, measured by their pairwise innerproduct. Each feature vector represents a single object, in our case a DTI voxel. For a set $\mathbf{S} = \mathbf{P} \cup \mathbf{N}$ of L objects o_j, the feature vector $\boldsymbol{f_i} = [d(o_i, o_1), ..., d(o_i, o_L)]$ representing o_i is computed by evaluating a distance measure between o_i and all other objects in $\mathbf{S}$.

As presented in Pekalska et al [17], a kernel $\mathbf{K}$ can be defined as a mapping of the feature vectors $\boldsymbol{f_i}$. The kernel matrix is then the inner-product between the feature vectors

$$K_{ij} \equiv < \boldsymbol{f}_i, \boldsymbol{f}_j > = \sum_k d(\mathbf{D_i}, \mathbf{D_k}) d(\mathbf{D_j}, \mathbf{D_k}) \tag{1}$$

where K_{ij} is the element in row i and column j of the kernel $\mathbf{K}$.

Each element in the kernel matrix effectively depends on all tensors in the training data. The kernel has high values for similar classes, but close to 0 for inter-class tensors. For geometric interpretation, consider that the inner product depicts the angle between two vectors. Now we have a kernel matrix, i.e., the set of all possible inner products, and it is symmetric and positive definite.

For a uniform behavior of the algorithm, without minding the scale of the used measures, a normalisation must be performed. We can normalise kernel matrices in such a way that the features lie on the surface of a unit hypersphere. This normalisation [18] can be done directly in the kernel as follows:

$$\widetilde{K}(f_i, f_j) = \frac{K(f_i, f_j)}{\sqrt{K(f_i, f_i) K(f_j, f_j)}} \tag{2}$$

A normalised kernel $\mathbf{K}$ from a distance measure m will be referred as $\mathbf{K^m}$.

2.3 Alignment

Christiani et al [19] proposed a method to assess the quality of a binary clustering. This measure, referred to as Kernel Target Alignment (KTA), depicts how good a kernel is with respect to a given set of labeled objects (the target) with the notion of good clustering, i.e., high similarity within clusters and low similarity between clusters. This notion is captured using the Frobenius inner product between these matrices. The Frobenius product between two matrices $\mathbf{V}$, $\mathbf{P}$ is defined as $< \mathbf{V}, \mathbf{P} >_F = \sum_{ij} v_{ij} p_{ij}$.

The *alignment* between two arbitrary kernels $\mathbf{K_1}$ and $\mathbf{K_2}$ is

$$A(\mathbf{K_1}, \mathbf{K_2}) = \frac{< \mathbf{K_1}, \mathbf{K_2} >_F}{\sqrt{< \mathbf{K_1}, \mathbf{K_1} >_F < \mathbf{K_2}, \mathbf{K_2} >_F}} \tag{3}$$

A target matrix is constructed from the set of n tensors $\mathbf{S}$. We define a vector of labels $\mathbf{y} \in \{-1, +1\}^n$ where 1 is the label for the positive set $\mathbf{P}$, and -1 for the

negative set $\mathbf{N}$. The target is then calculated using the matrix product $\mathbf{T} = \mathbf{y}^T\mathbf{y}$ and the alignment can now be expressed as

$$A(\mathbf{K}, \mathbf{T}) = \frac{< \mathbf{K}, \mathbf{T} >_F}{n\sqrt{< \mathbf{K}, \mathbf{K} >_F}}, \text{ since } < \mathbf{T}, \mathbf{T} >_F = n^2 \tag{4}$$

Linear combination of kernels: In machine learning, the problem of learning an adequate distance metric for the input space of data from a set of similar/dissimilar objects has been addressed in many studies in the recent years like Igel et al [14].

So far, we have a set of normalized kernels $\mathbf{K^m}$, one for each m measure. However, some kernels, i.e. some measures, may be more discriminative than others. Therefore, we introduce new parameters $w_m, m = 1, .., l$, with l as the number of distances to evaluate, and a new kernel will be constructed from the linear combination of the individual kernels:

$$\mathbf{K}(\overline{\mathbf{w}}) = \sum_{m=1}^{l} w_m \mathbf{K^m}, \text{ and } \sum_{m=1}^{l} w_m = 1, \ \overline{\mathbf{w}} = (w_1, ..., w_l), \ \forall_m w_m \geq 0 \tag{5}$$

Now, using the KTA measure, equation 4, with this kernel, and analysing the result of the alignment for different weights will result in assessing which linear combination of measures gives best discrimination for the analysed data. KTA is then a function of the weights w_m and its maximum will give the most appropriate measure, i.e., combination of measures. If the measures are not orthogonal to each other and do not represent specific characteristics of the tensor, a clear interpretation of the resulting weights cannot be given. Furthermore, an unique solution is not, necessarily, achieved. However, we still expect that the method will give a good balance of the measures and they will give good results although we cannot associate to the measures a clear interpretation.

2.4 Parameter Tuning using a Grid-Search based Method

The selection of weights is achieved by maximizing the alignment between the linear combination of kernels $\mathbf{K}$ and the target matrix $\mathbf{T}$

$$argmax_{\overline{w}}(A(\mathbf{K}(\overline{\mathbf{w}}), \mathbf{T})) = argmax_{\overline{w}} \left(\frac{< \mathbf{K}, \mathbf{T} >_F}{n\sqrt{< \mathbf{K}, \mathbf{K} >_F}} \right) \tag{6}$$

To determine the KTA's maximum, a grid-search in the parameter space spanned by the weights w_m is performed. The KTA is calculated at each point on the grid of parameter values, i.e., for each combination of w_m, with the above mentioned constraint, equation 5.

2.5 Region Growing

We apply our method for region growing segmentation as a proof of concept of the presented distance learning method. The weights, $\overline{w}$, that result from

the previous distance learning method are used to drive the Region Growing segmentation algorithm. The algorithm starts growing from the initially selected ROI. During the growing process the assignment of voxels is controlled by a voxel-to-neighborhood homogeneity predicate. A voxel is added to the region if its average weighted distance to the neighborhood, i.e., voxels already segmented and directly adjacent, is smaller than the average and standard deviation of the weighted distance between all pair of tensors in the seeding ROI.

3 Results

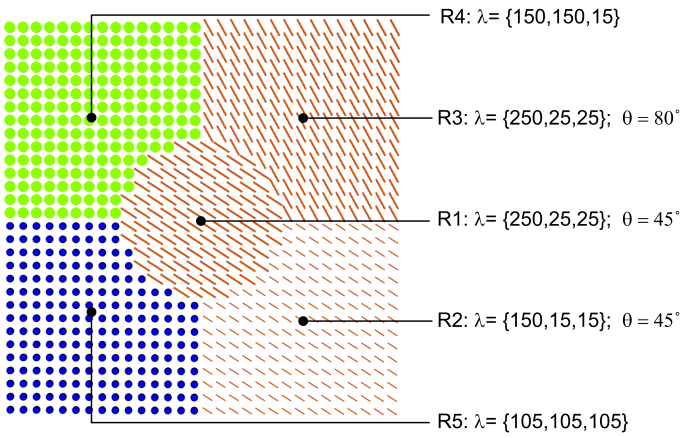

Fig. 3. Superquadric glyphs [20] showing the five distinct regions in a 30 × 30 tensor synthetic image. DTs have λ as eigenvalues.

The synthetic image shown in Figure 3 was designed so that the regions, despite having distinct DTs, share some properties with other region but are different to others., e.g., R1 has the same anisotropy as R2 and R3. With this synthetic data we intend to illustrate the behavior of the presented algorithm.

Considering this, to segment R1 an adequate distance must be chosen, for example d_{FA} would segment R1, R2 and R3. In these tests, the grid search method is done with $step = 0.1$. Choosing a ROI in R1, and randomly sampling 45 DTs, our algorithm estimates $w_{d_{L2}} = 1.0$ as the best discriminating distance. With these parameters, the region growing algorithm successfully segments only R1. Choosing a ROI between R1 and R2, the algorithm estimates a combination of two distances, $w_{d_{FA}} = 0.3$ and $w_{d_{ang1}} = 0.7$. As we can reason, what discriminates these two regions from the rest is their coherent orientation (45 degrees), distinct to R3, and FA, distinct to R4 and R5. The results were computed in a AMD Athlon 64 X2 Dual Core Processor 4800+ 2.41 GHz, with 3GB of RAM. The distance learning algorithm took about 8 seconds, per example.

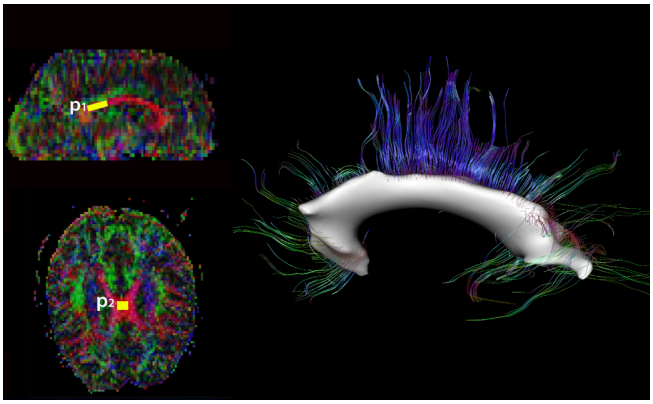

Fig. 4. Right: Fusion of the segmented *corpus callosum*, in a 128 × 128 × 30 DT volume, and the commissural fibers, colored using the typical RGB mapping of the main eigenvector. The estimated combination of distances is $d_{FA} = 0.5$ and $d_{ang1} = 0.5$. **Left:** P_1 and P_2 were used as positive ROIs.

Figure 4 shows the algorithm applied in a DTI brain dataset. Two positive ROIs were selected within the corpus callosum. Because the random sampling of the brain selected several DTs in the gray matter, the algorithm infers d_{FA} as the most suitable measure. This results in the segmentation of the white matter. In order to improve this, a white matter masking is done by sampling of DTs with a FA threshold, i.e., 50 DTs are used as negative examples if $FA > 0.70$. Then, the algorithm estimates $w_{d_{FA}} = 0.5$ and $d_{ang1} = 0.5$ as the best discriminating combination of measures. The obtained result does not capture entirely the corpus callosum, as can be seen by the commissural fibers manually clustered by physicians. The result is not surprising since the defined region of interest does not represent the span of DTs orientations. The distance learning algorithm took 10 seconds to compute.

In Figure 5 a positive ROI was selected within the right cingulum. With 30 random DTs taken with anisotropy $FA > 0.65$, the algorithm took 9 seconds to estimate $w_{d_{ang1}} = 1.0$ as the best measure, since the cingulum is a cylinder-like bundle with DTs coherently aligned.

4 Conclusions and Future Work

We proposed a distance learning method, based on kernel target alignment, for the optimization of Diffusion Tensor Imaging segmentation algorithms. As demonstrated, the method infers the most suitable distance(s) and parameters for the selected segmentation problem from the homogeneity/inhomogeneity characteristics of the data.

The used measures are of different nature and capture different aspects of the tensor data. Some measures isolate changes in individual degrees of freedom

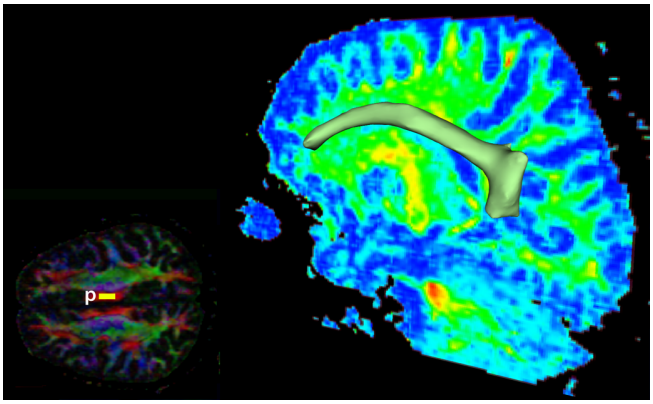

Fig. 5. Right: Right cingulum segmented with estimated $w_{d_{ang1}} = 1.0$, in a 231 × 172 × 131 DT volume, with **p** (yellow) as positive ROI, as seen in the **Left**. The sagittal plane, on the right, shows the FA map while the plane on the left shows the RGB color coding of the main eigenvector (red: sagittal plane; green: transverse plane; blue: coronal plane).

in the tensor data (e.g., difference in anisotropy). However, other measures, e.g., Log-Euclidean distance, d_{LE}, have no physiological significance and yield no clear intuition of distance between tensors. We present an initially flexible learning scheme that infers the combination of measures that give good results. Although, the resulting similarity measure will not be necessarily intuitive.

Furthermore the developed methods can be applied in other segmentation problems. For instance, Schultz [11] extended the use of structure tensors to diffusion tensor fields by combining Kindlmann's invariant gradients and rotation tangents [10,21]. The invariant's weights used to define the distance measure are set in an ad-hoc way. Our framework could help in the definition of the weights needed to tune the segmentation, based on the specific problem at hand.

In this paper, we presented a proof of concept with synthetic data and real data. This shows the potential of the presented method. However, doing a good evaluation is a challenging problem, starting in the definition of a good ground truth.

The grid search method used to find the optimal weights can be improved. As future work, we will investigate other, more computationally efficient, methods to solve the KTA optimization.

The present algorithm can be extended to HARDI (High Angular Resolution Diffusion Imaging) approaches to diffusion. It is still unknown what are the useful distances between two spherical functions such as DOT and Q-ball for applications like segmentation [22, 23].

Acknowledgements

This work was supported by: Fundação para a Ciência e a Tecnologia (FCT, Portugal) under grant SFRH/BD/24467/2005, and the Netherlands Organization for Scientific Research (NWO-VENI grant 639.021.407).

References

1. Basser, P.J., Mattiello, J., Lebihan, D.: MR diffusion tensor spectroscopy and imaging. Biophysical Journal **66** (1994) 259–267
2. Vilanova, A., Zhang, S., Kindlmann, G., Laidlaw, D.: An introduction to visualization of diffusion tensor imaging and its applications. In Weickert, J., Hagen, H., eds.: Visualization and Processing of Tensor Fields. Mathematics and Visualization. Springer (2005) 121–153
3. Zhukov, L., Barr, A.H.: Heart-muscle fiber reconstruction from diffusion tensor MRI. In: Proceedings of IEEE Visualization 2003, IEEE Computer Society (2003) 597–602
4. Melhem, E.R., Mori, S., Mukundan, G., Kraut, M.A., Pomper, M.G., van Zijl, P.C.: Diffusion tensor MR imaging of the brain and white matter tractography. American Journal of Roentgenology **178**(1) (2002) 3–16
5. Wang, Z., Vemuri, B.C.: DTI segmentation using an information theoretic tensor dissimilarity measure. IEEE Trans. Med. Imaging **24**(10) (2005) 1267–1277
6. Zhukov, L., Museth, K., Breen, D., Whitaker, R., Barr, A.: Level set modeling and segmentation of DT-MRI brain data. Journal of Electronic Imaging **12**(1) (2003) 125–133
7. Rousson, M., Lenglet, C., Deriche, R.: Level set and region based surface propagation for diffusion tensor mri segmentation. In Sonka, M., Kakadiaris, I.A., Kybic, J., eds.: ECCV Workshops CVAMIA and MMBIA. Volume 3117 of Lecture Notes in Computer Science., Springer (2004) 123–134
8. Moberts, B., Vilanova, A., van Wijk, J.J.: Evaluation of fiber clustering methods for diffusion tensor imaging. In: IEEE Visualization, IEEE Computer Society (2005) 9
9. Lenglet, C., Rousson, M., Deriche, R.: DTI segmentation by statistical surface evolution. IEEE Trans. Med. Imaging **25**(6) (2006) 685–700
10. Kindlmann, G., Ennis, D.B., Whitaker, R.T., Westin, C.F.: Diffusion tensor analysis with invariant gradients and rotation tangents. IEEE Trans. Med. Imaging **26**(11) (November 2007) 1483–1499
11. Schultz, T., Burgeth, B., Weickert, J.: Flexible segmentation and smoothing of DT-MRI fields through a customizable structure tensor. In: Advances in Visual Computing. Lecture Notes in Computer Science, Springer (2006) 455–464
12. Similarity Measures for Matching Diffusion Tensor Images. In: Proc. British Machine Vision Conference BMVC99. (1999)
13. Peeters, T., Rodrigues, P., Vilanova, A., ter Haar Romeny, B.: Analysis of distance/similarity measures for diffusion tensor imaging. In Laidlaw, D.H., Weickert, J., eds.: Visualization and Processing of Tensor Fields: Advances and Perspectives. Springer, Berlin (2008) in Press.
14. Igel, C., Glasmachers, T., Mersch, B., Pfeifer, N., Meinicke, P.: Gradient-based optimization of kernel-target alignment for sequence kernels applied to bacterial gene start detection. IEEE/ACM Trans. Comput. Biol. Bioinformatics **4**(2) (2007) 216–226

15. Schölkopf, S., Mika, B., Burges, S., Knirsch, C., Müller, P., Rätsch, K., Smola, G.: Input space vs. feature space in kernel-based methods. IEEE Transactions on Neural Networks **10**(5) (1999) 1000–1017
16. Haasdonk, B., Bahlmann, C.: Learning with distance substitution kernels. In Rasmussen, C.E., Bülthoff, H.H., Schölkopf, B., Giese, M.A., eds.: Pattern Recognition, 26th DAGM Symposium, August 30 - September 1, 2004, Tübingen, Germany, Proceedings. Volume 3175 of Lecture Notes in Computer Science., Springer (2004) 220–227
17. Pekalska, E., Paclik, P., Duin, R.: A Generalized Kernel Approach to Dissimilarity Based Classification. Journal of Machine Learning Research **2** (2001) 175–211
18. Graf, A.B.A., Borer, S.: Normalization in support vector machines. In: Proceedings of the 23rd DAGM-Symposium on Pattern Recognition, London, UK, Springer-Verlag (2001) 277–282
19. Cristianini, N., Shawe-Taylor, J., Kandola, J.: On kernel target alignment. Proceedings of the Neural Information Processing Systems, NIPS'01 (2002) 367–373
20. Kindlmann, G.: Superquadric tensor glyphs. In: Proceeding of The Joint Eurographics - IEEE TCVG Symposium on Visualization. (May 2004) 147–154
21. Kindlmann, G.L., Estépar, R.S.J., Niethammer, M., Haker, S., Westin, C.F.: Geodesic-loxodromes for diffusion tensor interpolation and difference measurement. In Ayache, N., Ourselin, S., Maeder, A.J., eds.: MICCAI (1). Volume 4791 of Lecture Notes in Computer Science., Springer (2007) 1–9
22. Descoteaux, M., Deriche, R.: Segmentation of q-ball images using statistical surface evolution. In Ayache, N., Ourselin, S., Maeder, A.J., eds.: MICCAI (2). Volume 4792 of Lecture Notes in Computer Science., Springer (2007) 769–776
23. Wassermann, D., Descoteaux, M., Deriche, R.: Diffusion maps clustering for magnetic resonance Q-Ball imaging segmentation. International Journal in Biomedical Imaging (2007) In press.